Title:

Gallium Distribution between Slag and Metal Phases during the Carbothermal Reduction of Bauxite

Authors:

Tomofumi Nakamura[1], Kouji Yasuda[1;*] and Tetsuya Uda[1]

Affiliations:

[1]Department of Materials Science and Engineering, Graduate School of Engineering, Kyoto University; Kyoto, 606-8501, Japan.

*Corresponding author. Email: yasuda.kouji.3v@kyoto-u.ac.jp, Tel: +81-75-753-5445

ORCID

Kouji Yasuda: https://orcid.org/0000-0001-5656-5359

Tetsuya Uda: https://orcid.org/0000-0002-2484-4297

Abstract

This article investigated the recoverability of the Ga in bauxite by carbothermal reduction. Currently, Ga is mostly manufactured from bauxite through Bayer process as a by-product of alumina, but it is worthwhile to consider alternative processes considering stricter environmental regulations and shortage of high-quality bauxite. This study focused on Pedersen process, which is the alumina production process consisted of carbothermal reduction and alkaline leaching. The metal and slag phases were prepared by carbothermal reduction of bauxite at 1873 K, and then aluminum in the slag was leached with (Na_2CO_3 + NaOH) solution at 348 K. Evaluation by ICP-AES and ICP-MS revealed that almost all Ga in bauxite was transferred to the metal phase, and the distribution to the slag phase was negligible in carbothermal reduction, which agrees with the thermodynamic consideration. These results suggest that the gallium recovery from pig iron is necessary to produce Ga in Pedersen process.

Keyword

Gallium, Bauxite, Carbothermal reduction, Distribution, Pig iron, Pyrometallurgy

1. Introduction

The demand for Gallium (Ga) is increasing in recent years as a semiconductor material such as GaN, GaAs, GaP, and CIGS ($Cu(In_xGa_{1-x})Se_2$) [1,2]. Worldwide production of Ga is only 550 tons per year in 2022, of which 540 tons are produced in China [1]. The abundance of Ga in the crust is 19 ppm, comparable to the amount of lead (Pb) [3]. Bauxite is an aluminum ore containing 10–100 ppm Ga, and approximately 90% of the global production of Ga is supplied as a byproduct in alumina production through the Bayer process as follows [3–5]. Ga contained in sphalerite in the range of 1–100 ppm is also recovered from the hydrometallurgical zinc (Zn) smelting process [3–6]. Here, along with the issues of the Bayer process, the Ga production process needs to be reconsidered under the environmental regulations that will become stricter in the future.

The Bayer process is the major current industrial production process of alumina, in which Al_2O_3 content in bauxite is leached into the strong alkaline leachate called Bayer liquor at an elevated temperature of 373–543 K and high pressure of 1–6 atm (approximately 1–6 × 10^5 Pa) [6]. Then, $Al(OH)_3$ is precipitated by lowering the temperature of the leachate, followed by calcination to produce alumina [8–10]. The process of Ga recovery from Al metallurgy was proposed by Goldschmidt in 1937. Ga is amphoteric metal as well as Al, and Ga component in bauxite is also leached in the Bayer process. Gallium accumulates in the Bayer liquor through the several cycles, reaching concentration between 100 and 200 mg L^{-1} [11]. By injecting carbon dioxide (CO_2) gas into the Bayer liquor, most of the AlO_2^- ions in the solution is removed as $Al(OH)_3$ precipitate.

$$AlO_2^-(aq) + CO_2(g) + 2H_2O(l) \rightarrow Al(OH)_3(s) + HCO_3^-(aq) \quad (1)$$

Ga component is recovered as $Ga(OH)_3$ precipitate from $Ga(OH)_4^-$ in solution by further CO_2 injection.

$$Ga(OH)_4^-(aq) + CO_2(g) \rightarrow Ga(OH)_3(s) + HCO_3^-(aq) \quad (2)$$

Then, alkaline solution dissolving $Ga(OH)_3$ and some $Al(OH)_3$ is obtained by adding NaOH solution. Metallic Ga is produced by electrowinning from alkaline solution containing purified $Ga(OH)_3$ [12].

The residue of the Bayer process is called red mud. It is a mixture of the leachate and solid particulate of undissolved Al_2O_3 and impurities such as Fe_2O_3, SiO_2, and TiO_2. The high alkalinity of red mud results in a high environmental impact and makes its disposal difficult. Red mud was mainly disposed of by ocean dumping until around 1960, but this was subsequently banned under the London Convention. Currently, solid-liquid separation is conducted by settling in sedimentation ponds and thickeners, and the precipitated solid is neutralized and then disposed of in landfills [13–15]. In 2010, however, catastrophic red mud spills from settling ponds occurred due to heavy rainfall and the flood destroyed the ecosystem and even claimed the lives of some people [13].

The Pedersen process is one of the alumina production processes, which was industrially operated in Norway between 1928 and 1969 [10,16,17]. Figure 1 shows a flowsheet of the Pedersen process. In the Pedersen process, bauxite, limestone, and coke are used as raw materials. By carbothermal reduction in an electric furnace at 1633–1773 K [16,17], the Fe_2O_3 in bauxite is reduced to pig iron, and the $CaO–Al_2O_3$ slag is formed. Al in the slag is leached by an alkaline solution consisting of Na_2CO_3 and NaOH, and then, $Al(OH)_3$ is precipitated by blowing carbon dioxide into the leachate, and Al_2O_3 is produced by calcination. Alkaline leaching residue called grey mud is a $CaO–SiO_2$ slag, which can be used as cement material. One of the advantages of the Pedersen process is a conversion of impurities into harmless industrial raw materials such as pig iron and grey mud instead of red mud. Another advantage is the wide acceptability of bauxite. While only high-quality bauxite is used in the Bayer process, bauxite with high SiO_2 composition can be used in the Pedersen process. This is because alkaline leaching is performed at lower pH, pressure and temperature in the Pedersen process than the Bayer process, and SiO_2 in the $CaO–SiO_2$ slag has a lower

solubility to alkaline solution.

The Pedersen process should be reconsidered as the next-generation and environmentally-friend alumina production process under stricter environmental regulations to achieve a sustainable society. In particular, the advantage of the Pedersen process over the Bayer process will increase because alarming situations are anticipated in the future such as the rising cost of raw materials due to a shortage of high-quality bauxite and that of processing red mud due to stricter environmental regulations. Actually, although the Pedersen process has been out of operation since 1969 [16], a project to review the process started in Europe in 2017, and a pilot plant was constructed [18].

As far as the best knowledge of the authors, there have been no report on the recovery of Ga as a byproduct of the Pedersen process. Thus, this study experimentally investigated the distribution of Ga between metal and slag phases by inductively coupled plasma atomic emission spectroscopy (ICP-AES) and inductively coupled plasma mass spectrometry (ICP-MS) to evaluate the possibility of Ga recovery.

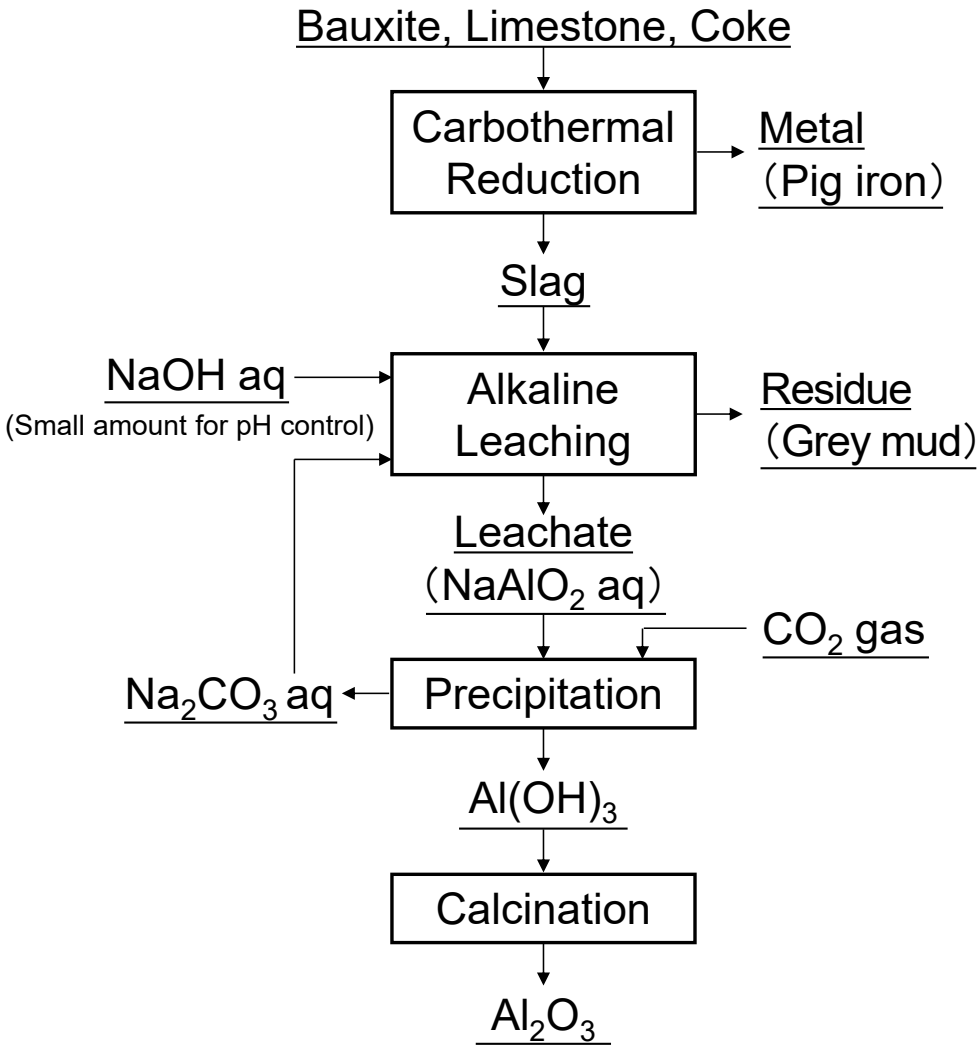

Figure 1 Flowchart in the Pedersen process for alumina production.

2. Experimental

2.1 Carbothermal reduction of bauxite

Carbothermal reduction was performed to a mixture of bauxite (Tokyo Science Co., Ltd., from Australia), $CaCO_3$ powder (Nacalai Tesque, Inc., purity: 99.5 %), and graphite powder (Fujifilm Wako Pure Chemical Corp., purity: 98.0 %). The XRD pattern and the WDS analytical result are shown in Fig. S-1 in supplemental information. Composition of the bauxite is as follows; $Al(OH)_3$: 76.08 mass%, Fe_2O_3: 14.67 mass%, SiO_2: 5.01 mass%, TiO_2: 4.23 mass%, and Ga: 21.7 ppm. Other trace metal impurities identified in

WDS were Cu, Zn, and K. Bauxite was pre-milled by a mortar and pestle, and was passed through a sieve with 500 μm mesh opening. The addition amount of $CaCO_3$ was determined to be a sum total of the ratio to Al_2O_3 and that to SiO_2 in the bauxite. The ratios calculated based on the literatures are Al_2O_3:CaO = 45:55 (molar ratio) [19] and SiO_2:CaO = 1:2 (molar ratio) [16]. The amount of graphite was adjusted to the ratio of Fe_2O_3:C = 1:2.25 (molar ratio) [19]. A graphite crucible (As One Corp., $\phi 30\times30^{h}\times2^{t}$ mm) also worked as a reductant in addition to the graphite powder. Approximately 3 g of the above-mixed powder was placed in a die (carbon steel, SK-3, inner diameter: 17 mm) and compressed at 4 kN by a uniaxial pressing machine (NPa System Co., Ltd., NT-100H) to form a pellet with a thickness of approximately 4 mm. In Exp. #1, pellet and powder samples with a total mass of 12.007 g were filled into the graphite crucible. In Exp. #2, 4.907 g of iron block (Kojundo Chemical Laboratory, Co., Ltd., purity: 99.99%) was also set in addition to the powder and pellet so that the metal product forms a large block which enables easy separation of the metal and slag phases. Masses of the loaded samples in Exp. #1 and #2 are summarized in Table 1. The graphite crucibles were placed in an alumina crucible (Nikkato Corp., SSA-S, $90\times55\times33^{h}$ mm) and placed in a horizontal tube furnace (Starbar Japan Co., Ltd., furnace size: $\phi 80\times1000$ mm). The carbothermal reduction was conducted at 1873 K for 1 hour in an Ar flow of 200 sccm.

Table 1 Mass of loaded sample in the carbon crucible in the carbothermal reduction experiment

Chemical		Exp. #1	Exp. #2
Mass (g)	Bauxite	5.476	3.286
	$CaCO_3$	6.319	3.793
	Graphite	0.212	0.127
	Iron	not added	4.907
	Total	12.007	12.113

Sample collected in Exp. #1 was broken with a hammer in a plastic bag and its cross-section was observed. The volume portion of metal phase was small. The sample was further crushed into about 5 mm in size,

ground by a mortar and pestle, and passed through a sieve with 500 μm mesh opening. It was then separated into magnetic and non-magnetic powders by a ferrite magnet enclosed in a plastic wrap. In Exp. #2, the collected sample was hammered to separate into slag and metal. The recovered metal was then cut using metal scissors to obtain grains about 3 mm in size and 0.2–0.5 g in mass.

2.2 Alkaline leaching of the slag

The leachate was 120 g L^{-1} Na_2CO_3 + 7.0 g L^{-1} NaOH solution prepared from Na_2CO_3 (Nacalai Tesque, Inc., purity: 99.7 %) and NaOH (Nacalai Tesque, Inc., purity: 97.0 %) [20]. Approximately 0.5 g of the slag and 10 g of (Na_2CO_3 + NaOH) solution were added to two Teflon containers. After putting the Teflon lid, each Teflon container was sealed in stainless container (OM LAB-TECH Co., Ltd., sealed crucible MR-28). Alkaline leaching was conducted by holding stainless container in a convection oven at 348 K for 2 hours. After heat-treatment, the oven was turned off, and its door was opened to cool for 30 min. The sample in the container was filtered using a filter paper (5C, 110 mm, particle retention: 1 μm) and separated into alkaline leaching solution and residue. The residue was dried in the oven at 348 K for 16 hours in air.

2.3 Sample analysis

Phase identification was performed by X-ray diffraction (XRD) analysis using X'pert Pro (Panalytical Ltd., Cu-Kα, 45 kV, 40 mA). Solid composition and liquid concentration in each sample were determined by inductively coupled plasma (ICP) measurement with ICP-MS (Agilent Technologies, Inc., Agilent 7700s) for Ga, and ICP-AES (SII Nanotechnology, SPS 3500) for other elements. Since Ga content measured with ICP-AES was affected by background spectrum mainly associated with Fe peaks, it was evaluated with ICP-MS.

For the ICP measurement of the products obtained by carbothermal reduction, approximately 0.5 g of each product was subjected to acid leaching with 2.58 mol L^{-1} HCl at an L/S mass ratio of 20.0. Specific

conditions are shown in Table S-1 and S-2 in supplemental information. In Exp. #1, each powder and HCl solution were placed in a centrifuge tube and leached for 1 hour without agitation. In Exp. #2, due to the large size of the metal (grains about 3 mm), the sample was held in the solution for 24 hours to complete the reaction. The analysis for the alkaline leaching residue was conducted by an alkaline fusion in a platinum crucible using 0.5 g of the sample, 3.0 g of Na_2CO_3 (Nacalai Tesque, Inc., purity: 99.7 %), and 1.0 g of H_3BO_3 (Fujifilm Wako Pure Chemical Corp., purity: 99.5 %) [21,22]. The platinum crucible placed on an alumina square tray (Nikkato Corp., SSA-S, 60 × 40 mm) was set in a horizontal electric furnace (Asahi Rika Manufacturing Ltd., ARF1110-300-80KC) in an Ar atmosphere at 1173 K for 2.5 hours. The sample solution was prepared by dissolving the obtained product in a mixed solution of 15 ml concentrated HCl (Nacalai Tesque, Inc., purity: GR (35–37 %)) and 15 ml deionized water with removing the $B(OH)_3$ precipitate by filtration.

3. Results and discussion

3.1 Carbothermal reduction and alkaline leaching

Fig. 2(a) and (b) show the photographs of the samples before and after the carbothermal reduction in Exp. #1, respectively. The color of mixed powder changes from reddish-brown to gray. As a cross-section of sample after the reaction in Exp. #1 shows in Fig. 2(c), two phases are observed: the metal phase with 1–2 mm in size and a metallic luster, and the slag phase with a gray color. The metal phase is unevenly distributed at the bottom of the graphite crucible, which is a reasonable behavior for a greater density of pig iron than that of the $CaO–Al_2O_3–SiO_2$ slag. Meanwhile, in the carbothermal reduction with pure iron in Exp. #2, formation of a large metal block and the separation of slag and metal phase are observed as shown in Fig. 2 (d).

In Exp. #1, a magnetic powder (sample #1M: 0.716 g) and a non-magnetic powder (sample #1NM: 6.025 g) were obtained by crushing, grinding, and magnetic separation. During crushing with a hammer, the

plastic bag was punctured and some samples were spilled out, thus all of the sample could not be recovered. The yield of the recovered sample masses was 92.0 % against the estimated mass (7.330 g) when assuming reaction that the formation of Al_2O_3, CaO, and Fe from $Al(OH)_3$, $CaCO_3$, and Fe_2O_3, respectively, and complete consumption of carbon powder. Fig. 3 shows the XRD patterns of samples #1M and #1NM. For sample #1NM, $Ca_3Al_2O_6$ and $Ca_5Al_6O_{14}$ are identified. On the other hand, for sample #1M, $Ca_3Al_2O_6$ and $Ca_5Al_6O_{14}$ are also identified in addition to Fe_3C and Fe. Although sample #1M has a magnetic property and metallic luster, this XRD result indicates that sample #1M contains slag phases due to their adherence to metal. In alkaline leaching at 348 K for 2 h, 0.993 g of an alkaline leaching residue (sample #1NM-R) was recovered from 1.000 g of sample #1NM. The alkaline leaching solution (sample #1NM-S) was also recovered.

In Exp. #2, masses of the slag and metal were 3.815 g and 5.256 g, respectively. According to same assumption in Exp.#1, the yield of the recovered sample masses was almost 100%. The slag powder obtained by crushing, grounding, and classification less than 500 μm hardly stuck to the magnet. The metal phase was not contained in the sample recovered as slag phase.

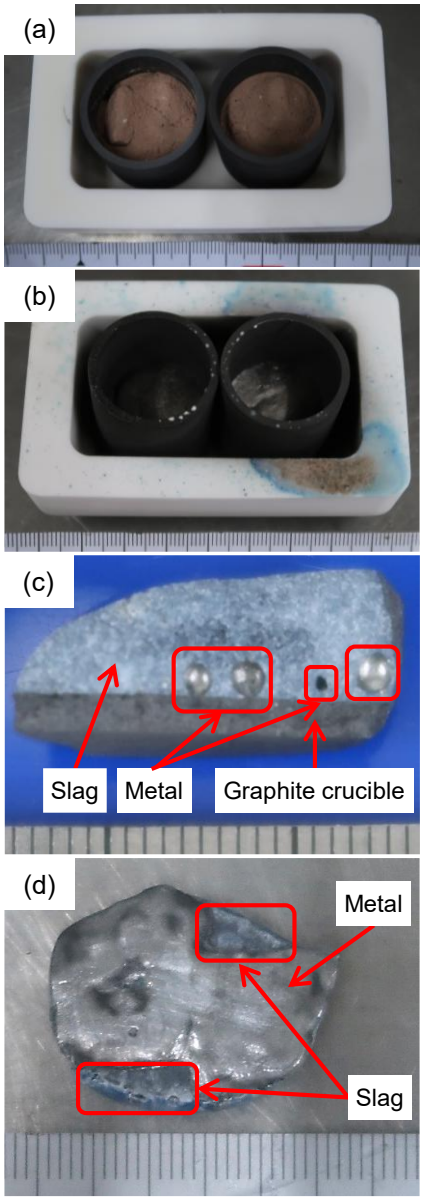

Figure 2 Photographs of the sample (a) before and (b) after carbothermal reduction in Exp. #1, (c) cross-section of the sample after carbothermal reduction in Exp. #1, and (d) the sample after carbothermal reduction (view from the bottom) in Exp. #2

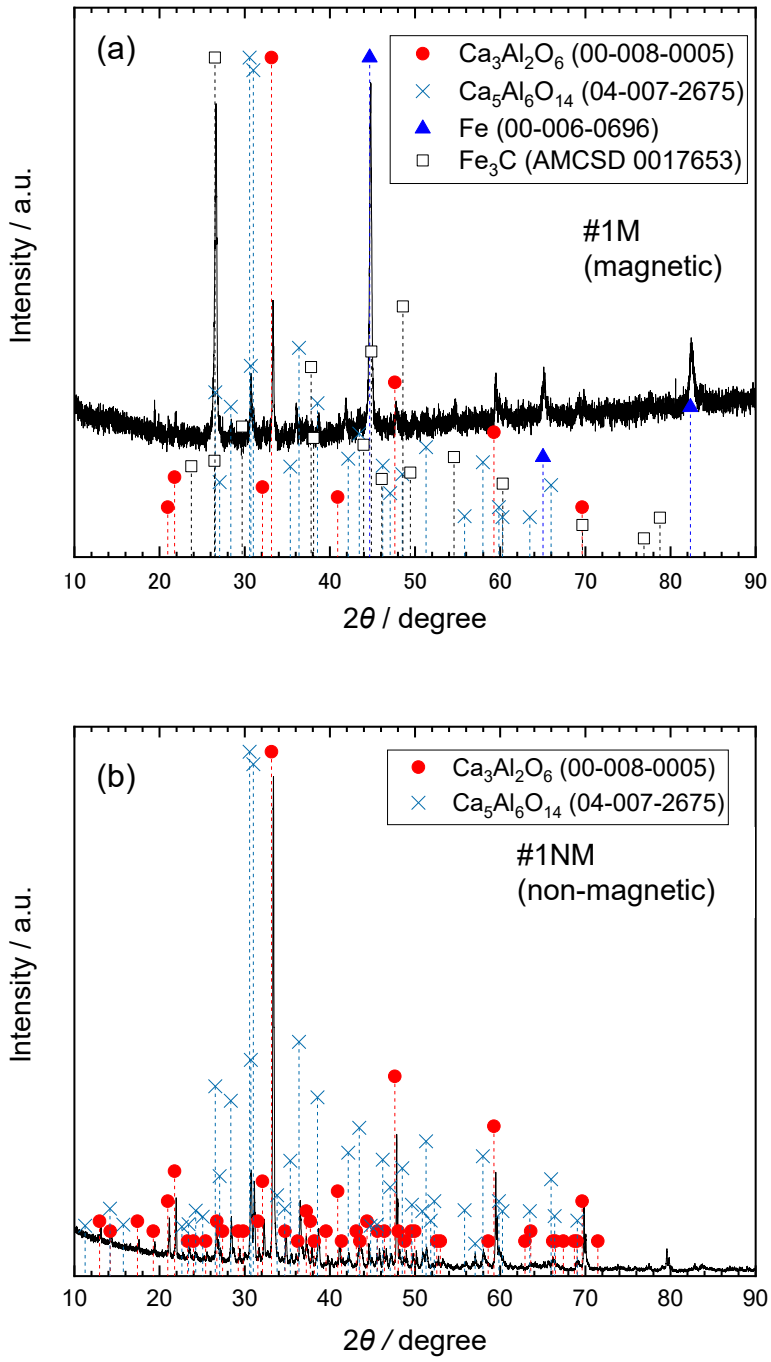

Figure 3 XRD patterns of (a) the magnetic powders (#1M) and (b) non-magnetic powders (#1NM) recovered in carbothermal reduction in Exp. #1.

3.2 Determination of elemental concentrations by ICP analysis

3.2.1 Products of carbothermal reduction

To estimate the amount of slag phase adhered to the metallic phase, a part of the sample was leached with HCl solution. After immersing in HCl solution at room temperature, metal phase was completely dissolved and a part of slag phase remained as residue. Table 2 shows the results of ICP analysis of the HCl leachates for samples #1M and #1NM. The elemental compositions of the HCl-soluble components in each sample, calculated from results of ICP analysis, were also listed. Sample #1M with strong magnetism has high composition of Fe at 57.4 %, which agrees to the report that the metal phase in the Pedersen process is pig iron. Al composition in samples #1M was 3.80 %. It is difficult for the aluminum oxides to be thermodynamically reduced by carbothermal reduction. This Al content, therefore, should correspond to the amount of slag phase. The mixing ratio of metal and slag phases in sample #1M is estimated with comparing the result of leaching experiment of sample #1NM. Here, three assumptions were employed: (1) Al does not transfer to the metal phase and its composition in the metal phase is zero, and (2) the elution behavior of Al content of the slag phase in sample #1M was the same for sample #1NM, that is, the Al content in the solution was proportional to the mass of slag regardless of whether it was in sample #1M or #1NM. (3) The mass of carbon in cementite can be ignored. The estimated mass ratio of slag phases in sample #1M was 22 %, and rest of 78 % is assumed to be metal phase. Using this mass ratio and the result of ICP analysis of samples #1M and #1NM about Fe and Ga, the compositions of both elements in the metal phase are estimated. Ga composition in metal phase is 2.7×10^2 ppm and Fe composition is 73.6 %. The values of the compositional estimate may be smaller than actual values due to the effect of the ignored carbon content and adsorption of Fe and Ga ion on the residue during the ICP analysis.

Table 2 ICP analytical results of the products of carbothermal reduction in Exp. #1

		Al	Fe	Si	Ti	Ga[d]
Magnetic powders (sample #1M)	ICP solution, c_1 (ppm)	3.81[b]	57.51[b]	3.15[c]	3.34	0.21[c]
	HCl-soluble component, c_2[a] (ppm) in solid	3.80×10^4 (3.80 %)	5.74×10^5 (57.4 %)	3.14×10^3	333	2.1×10^2
Non-magnetic powders (sample #1NM)	ICP solution, c_1 (ppm)	17.3[b]	1.57	0.114[b]	1.72	0.0012[c]
	HCl-soluble component, c_2[a] (ppm) in solid	1.73×10^5 (17.3 %)	157	1.14×10^3	172	1.2

a: $c_2 = \frac{50}{0.501} \times c_1 \times n$, where n means dilution ratio, 50 means volume of ICP solution (ml), and 0.501 means sample mass (g) dissolved in ICP solution. b: Measured 100 times diluted solution. c: Measured 10 times diluted solution. d: Measured with ICP-MS.

In Exp. #2, the metal phase was obtained as a lump and analyzed at three locations. Table 3 shows the results of the ICP analysis of the HCl solution of sample in Exp. #2 and the elemental compositions of the HCl-soluble components in each phase. The analysis was limited to three elements of Al, Fe, and Ga. In Exp. #2, the composition of Ga in the metal phase is about 15 ppm. Similar to Exp. #1, the analytical values may be smaller than actual due to adsorption on carbon residue.

Table 3 ICP analytical results of the metal products of carbothermal reduction in Exp. #2

			Al	Fe[e]	Ga[f]
Metal	#2-1	ICP solution, c_1 (ppm)	0.63	78.6	0.016[f]
		HCl-soluble component, c_2[a] (ppm) in solid	64	7.97×10^5 (73.6 %)	16
	#2-2	ICP solution, c_3 (ppm)	0.37	84.2	0.015[f]
		HCl-soluble component, c_4[b] (ppm) in solid	37	8.45×10^5 (84.5 %)	15
	#2-3	ICP solution, c_5 (ppm)	Not measured		0.015[f]
		HCl-soluble component, c_6[c] (ppm) in solid			15
Slag		ICP solution, c_7 (ppm)	17.2 [e]	0.20	0.001[f]
		HCl-soluble component, c_8[d] (ppm) in solid	1.72×10^5 (32.5 % as Al_2O_3)	20 (26 ppm as FeO)	1 (1 ppm as Ga_2O_3)

a: $c_2=\frac{50}{0.493}\times c_1\times n$ b: $c_4=\frac{50}{0.498}\times c_3\times n$ c: $c_6=\frac{50}{0.492}\times c_5\times n$ d: $c_8=\frac{50}{0.501}\times c_7\times n$

e: Measured 100 times diluted solution. f: Measured 10 times diluted solution with ICP-MS.

3.2.2 Products of alkaline leaching

The results of ICP analysis of the alkaline leaching solution and residue in Exp. #1 are shown in Table 4. Al is the most abundant element among the analyzed elements both for alkaline leaching solution (0.301 %, #1NM-S) and residue (11.3 %, #1NM-R). Although Al leaching was confirmed to be almost completed in

previous reports [23], its extraction ratio in this study was not sufficient, probably because stirring was not performed in this study and $Ca_3Al_2O_6$ phase was not highly reactive to (Na_2CO_3 + NaOH) solution. Ga concentration in alkaline leaching solution and residue are below detection limit and 0.56 ppm, respectively.

Table 4 ICP analytical results of the products of alkaline leaching in Exp. #1

		Al	Fe	Si	Ti	Ga[f]
Alkaline leaching solution (#1NM-S)	ICP solution, c_1 (ppm)	12.1[d]	< 0.002	32.3[e]	< 0.001	$< 8\times10^{-6}$
	Leaching solution, c_2[b] (ppm) in leachate	3.01×10^3 (0.301 %)	< 0.005	80.5	< 0.003	$< 3\times10^{-5}$
Alkaline leaching residue[a] (#1NM-R)	ICP solution, c_3 (ppm)	11.3[d]	4.60[e]	1.36[d]	1.33[d]	0.00056[e]
	Residue, c_4[c] (ppm) in solid	1.13×10^5 (21.4 % as Al_2O_3)	4.60×10^3 (0.6 % as FeO)	1.36×10^4 (2.9 % as SiO_2)	1.33×10^4 (2.2 % as TiO_2)	0.56 (0.8 ppm as Ga_2O_3)

a: The solution for analysis was prepared by alkaline fusion. b: $c_2 = \frac{50}{20.1}\times c_1\times n$, where 20.1 means leachate mass. c: $c_4 = \frac{50}{0.500}\times c_3\times n$ d: Measured 100 times diluted solution. e: Measured 10 times diluted solution. f: Measured with ICP-MS.

3.3 Phase transfer of Ga considered in terms of mass balance

In this section, mass balance of Ga into the metal phase and slag phase in the process of the carbothermal reduction is evaluated.

Input: As mentioned in section 2.1, Ga composition of the bauxite used in this study is 21.7 ppm. In Exp.

#1, 5.476 g of bauxite in which 0.119 mg of Ga was contained and 6.319 g of $CaCO_3$ were used for the carbothermal reduction.

Output: First, the recovery yield of the reduction experiment was compensated. If the yield of each phase is 100 %, the sample mass after reduction is estimated to be 7.330 g. However, the yield was 92.0 %. 0.716 g for the magnetic powder (sample #1M) and 6.025 g for the non-magnetic powder (sample #1NM) were recovered. Second, the weight of metal and slag phases were calculated since sample #1M was estimated to be a mixture of metal and slag phases at 78:22 mass ratio and the sample #1NM was solely composed to the slag phase. Masses of metal and slag phase generated during carbothermal reduction were roughly estimated as follows.

metal phase: $0.716 \times 0.78 / 0.92 = 0.607$ g (3)

slag phase: $(6.025 + 0.716 \times 0.22) / 0.92 = 6.720$ g (4)

where the spilled sample during crushing with a hammer was assumed to have nearly identical composition to the sample that was not spilled. Third, as Ga composition in metal phase is 270 ppm, Ga amount transferred to the metal phase is estimated to be 0.16 mg. Fourth, the weight of Ga transferred to the slag phase was obtained as the total amount in the alkaline leaching solution and residue. Regarding in the alkaline leaching solution, transferred Ga is less than 3×10^{-6} mg calculated from slag mass of 6.720 g and the analytical concentration less than 8×10^{-6} ppm for 50 mL of the solution obtained by leaching 1.000 g of the slag. The amount of Ga in the alkaline leaching solution can be ignored. Transferred Ga to the alkaline leaching residue is 3.7×10^{-3} mg calculated from Ga composition of 0.56 ppm and mass of 6.673 g estimated by assuming alkaline leaching of the total amount of slag (6.720 g).

Mass balance: The mass balance of Ga between metal and slag is listed in Table 5. The result in Exp. #2 is also presented in Table 5. The estimated Ga transfer ratio in the carbothermal reduction of Exp. #1 when

the total is normalized as 100% from the values in Table 5 is shown in Fig. 4, indicating that the majority of the Ga content in bauxite is transferred to the metal phase. The cause of the Ga transfer ratio exceeding 100% could be that the mass of the metal phase was overestimated based on the assumption in 3.2.1, or accurate analysis was difficult for Exp.#2 because of a very small amount of Ga by addition of pure iron. Our result agrees with the report that Ga transfers to pig iron in the carbothermal reduction in blast furnace [24]. According to Ref. [25], Ga metal contained in pig iron evaporates under reduced pressure at 1973 K. It is desirable to develop various recovery methods of Ga from pig iron such as vacuum smelting.

Table 5 Transfer ratio of Ga during the carbothermal reduction in the Pedersen process. The values include the uncertainties of the assumptions discussed in Exp.#1 and difficulties of accurate analysis of very small amount of Ga by addition of pure iron in Exp. 2.

		Metal	Slag
Ga composition (ppm)	Exp. #1	270	*ca* 0.56
	Exp. #2	15	*ca* 0.61
Transfer ratio (%)	Exp. #1	130	*ca* 3.1
	Exp. #2	110	*ca* 3.3

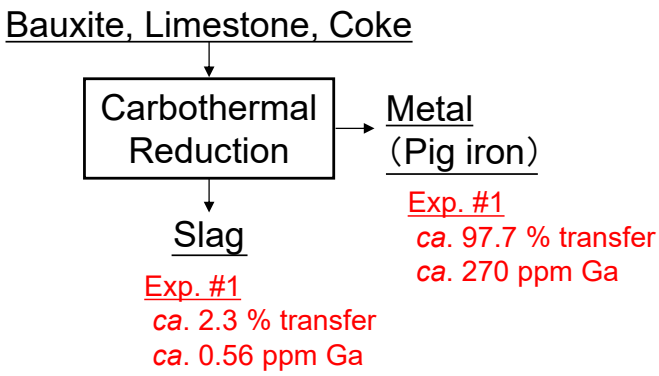

Figure 4 Transfer ratio and concentration of Ga in the products of the carbothermal reduction (Exp. #1).

Thermodynamics: To thermodynamically analyze the Ga distribution ratio between metal and slag phase in the carbothermal reduction, equilibrium (5) was evaluated at 1873 K.

$$4\mathrm{Ga}\ (l)_{\text{in metal}} + 3\mathrm{O_2}\ (g) = 2\mathrm{Ga_2O_3}\ (l)_{\text{in slag}} \tag{5}$$

$$\Delta G^{\circ} = -940.248\ \mathrm{kJ\ mol^{-1}}\ [26]$$

The standard states of Ga(l) and Ga_2O_3(l) are both considered pure liquids. The activity coefficient of Ga in molten iron, $\gamma^{\circ}_{\mathrm{Ga}}$, was calculated from the Redlich-Kister model parameters in subregular solution model ($^{0}L_{\mathrm{Fe,Ga}} = -86{,}500 + 18 \times T$ (J mol^{-1}), $^{1}L_{\mathrm{Fe,Ga}} = -15{,}363 + 3.5 \times T$ (J mol^{-1}), $^{2}L_{\mathrm{Fe,Ga}} = -13{,}000$ (J mol^{-1}) [27]) with assuming binary liquid of Fe–Ga. Assuming that the Henry's law is applicable to Ga concentration of 0.1 mol % in molten iron at 1873 K, $\gamma^{\circ}_{\mathrm{Ga}}$ is calculated from mole fraction, x, and the interaction parameter, Ω, obtained by the Redlich-Kister polynomial as follows.

$$\Omega = {}^{0}L_{\mathrm{Fe,Ga}}\,(x_{\mathrm{Fe}} - x_{\mathrm{Ga}})^{0} + {}^{1}L_{\mathrm{Fe,Ga}}\,(x_{\mathrm{Fe}} - x_{\mathrm{Ga}})^{1} + {}^{2}L_{\mathrm{Fe,Ga}}\,(x_{\mathrm{Fe}} - x_{\mathrm{Ga}})^{2}$$

$$= -74.524\ \mathrm{kJ\ mol^{-1}} \tag{6}$$

$$\gamma^{\circ}_{\mathrm{Ga}} = \exp(\Omega \cdot (1 - x_{\mathrm{Ga}})^2/\mathrm{RT})$$

$$= 0.008 \quad (7)$$

The activity coefficient of Ga in the Fe–C–Ga solution, γ_{Ga}, is estimated under carbon saturation condition, saturated solubility of C to Fe is about 20 mol %, assuming the following Wagner's approximation.

$$\ln\gamma_{\mathrm{Ga}} = \ln\gamma^{\circ}_{\mathrm{Ga}} + \varepsilon^{(\mathrm{Ga})}_{\mathrm{Ga}} x_{\mathrm{Ga}} + \varepsilon^{(\mathrm{C})}_{\mathrm{Ga}} x_{\mathrm{C}}$$

$$= -4.83 + 1.0\times10^{-3}\varepsilon^{(\mathrm{Ga})}_{\mathrm{Ga}} + 0.2\varepsilon^{(\mathrm{C})}_{\mathrm{Ga}} \quad (8)$$

where $\varepsilon^{(\mathrm{Ga})}_{\mathrm{Ga}}, \varepsilon^{(\mathrm{C})}_{\mathrm{Ga}}$ are interaction coefficients of Ga–Ga and Ga–C, and $\varepsilon^{(\mathrm{C})}_{\mathrm{Ga}}$ is reported as 2.725 [28]. The absolute value of general interaction coefficient is at most 10, and the second term in equation (8) can be ignored. As a result, $\ln\gamma_{\mathrm{Ga}}$ is calculated as −4.29, and γ_{Ga} is estimated as 0.014. The activity coefficient of Ga_2O_3 in the slag, $\gamma^{\circ}_{\mathrm{Ga_2O_3}}$ obtained by thermodynamic calculation software FactSage 6.4 [29] as 2.7×10^{-3} at 1×10^{-3} mol %Ga_2O_3 in slag (composition of 65.4 mol %CaO–22.3 mol %Al_2O_3–12.3 mol %SiO_2, expected from the raw material composition). Consider the endpoint of the carbothermal reduction as the equilibrium between C (*s*, graphite) and CO (g) at 0.01 bar (10^3 Pa) or 10^{-5} bar (1 Pa), as exampled partial pressures in Ar flow at 1873 K in reaction (9), the oxygen partial pressure, $p_{\mathrm{O_2}}$, in this case can be calculated according to equation (10).

$$\mathrm{C}(s, \text{graphite}) + 1/2\ \mathrm{O_2}(g) = \mathrm{CO}(g) \quad (9)$$

$$\Delta G^{\circ} = -275.374\ \mathrm{kJ\ mol^{-1}}\ [26]$$

$$p_{\mathrm{O_2}} = \exp((2\Delta G^{\circ} + RT\ln p_{\mathrm{CO}}{}^2 - RT\ln a_{\mathrm{C}}{}^2)/RT) \quad (10)$$

where the activity of carbon, a_C, is unity. The oxygen pressure is 4.4×10^{-20} bar and 4.4×10^{-28} bar for CO (g) at 0.01 bar (10^3 Pa) and 10^{-5} bar (1 Pa), respectively. Given the above γ_{Ga} and $\gamma^{\circ}_{Ga_2O_3}$, the value of $\frac{x_{Ga}{}^2}{x_{Ga_2O_3}}$ is calculated from equation (5) to be 5.9×10^{16} and 5.9×10^{28} at p_{O_2} $= 4.4\times10^{-20}$ and 4.4×10^{-28} bar, respectively. These results indicate that almost all of the Ga is thermodynamically transferred to the metal phase in carbothermal reduction.

In addition, thermodynamic considerations were conducted for the possibility of Ga transfer to the gas phase at 1873 K. As gaseous species, Ga(*g*) and suboxide Ga_2O(*g*) were evaluated. The standard Gibbs energy of formation ΔG_f° of Ga(*g*) and Ga_2O(*g*) at 1873 K are 63.384 kJ mol^{-1} and −196.401 kJ mol^{-1} [26]. First, considering evaporation of Ga(*g*) from Fe–C–0.1 mol % Ga(*l*) under carbon saturation condition, where γ_{Ga} is 0.014 calculated above, the vapor pressure of Ga(*g*), p_{Ga}, is estimated as 2×10^{-7} bar. Second, considering evaporation of Ga_2O(*g*), at the oxygen partial pressure under CO(0.01 bar)/C or FeO(*l*)(a_{FeO} = 0.1)/Fe(*l*) equilibrium, p_{Ga_2O} is calculated to be 1×10^{-14} and 2×10^{-12} bar, respectively. These results suggest that Ga transfer to the gas phase hardly occur during carbothermal reduction in this study. However, the vacuum evaporation at higher temperature might be possible as like introduced in Ref. [25].

4. Conclusions

The phase transfer of Ga in the Pedersen process was experimentally investigated to evaluate the possibility of Ga recovery as a byproduct of alumina. This research experimentally and thermodynamically revealed that most of the Ga content in bauxite is transferred to the metal phase of pig iron in the carbothermal reduction process, although there remains an error in balance owing to the low concentration of Ga which requires more strict evaluation using a larger amount of materials used. Therefore, when the alumina production process is replaced from the Bayer process to the Pedersen process, development of a recovery process of dilute Ga from pig iron is necessary.

Disclosure Statement

There are no conflicts to declare.

References

1. Mineral Commodity Summaries 2023. United States Geological Survey. https://pubs.usgs.gov/periodicals/mcs2023/mcs2023.pdf Accessed 2 March 2023
2. Ramanujam J, Singh U P (2017) Copper indium gallium selenide based solar cells – a review. Energy & Environmental Science 10:1306–1319. https://doi.org/10.1039/c7ee00826k
3. Japan Oil, Gas and Metals National Corporation (JOGMEC) (2009) Rare Metal Handbook 2009. Kinzoku Jihyo, Tokyo.
4. Habashi F (Editor) (1997) Handbook of Extractive Metallurgy, Wiley VCH.
5. Zhang L, Xu Z (2018) A critical review of material flow, recycling technologies, challenges and future strategy for scattered metals from minerals to wastes. Journal of Cleaner Production 202: 1001–1025. https://doi.org/10.1016/j.jclepro.2018.08.073
6. Fupeng L, Zhihong L, Yuhu L, Wilson B P, LundströmM (2017) Recovery and separation of gallium(III) and germanium(IV) from zinc refinery residues: Part I: Leaching and iron(III) removal. Hydrometallurgy 169: 564–570. https://doi.org/10.1016/j.hydromet.2017.03.006
7. Power G, Gräfe M, Klauber C (2011) Bauxite residue issues: I. Current management, disposal and storage practices. Hydrometallurgy 108:33–45. https://doi.org/10.1016/j.hydromet.2011.02.006
8. Hind A R, Bhargava S K, Grocott S C (1999) The surface chemistry of Bayer process solids: a review. Colloids and Surfaces 146: 359–374. https://doi.org/10.1016/S0927-7757(98)00798-5
9. Misra C, White E T (1971) Crystallisation of Bayer Aluminum trihydroxide. Journal of Crystal Growth 8:172–178. https://doi.org/10.1016/0022-0248(71)90138-2
10. Safarian J, Kolbeinsen L (2016) Sustainability in alumina production from bauxite. 2016 Sustainable

Industrial Processing Summit and Exhibition 5:75–82.

11. Chaves A P, Abrao A, Avristcher W (2000) Gallium recovery as a by-product of bauxite. Light Metals, 2000, 891–896

12. Zhao Z, Yang Y, Xiao Y, Fan Y (2012) Recovery of gallium from Bayer liquor: A review. Hydrometallurgy 125–126:115–124. https://doi.org/10.1016/j.hydromet.2012.06.002.

13. Osamu I (2011) Hungary sangyo-haikibutu ryuushutu jiko ni miru touo to EU no kyokai. Kyokai Kenkyu, 2:149–172. https://src-h.slav.hokudai.ac.jp/publictn/JapanBorderReview/no2/07_ieda.pdf. Accessed 24 May 2022

14. Toshihiro K, Tadato M (1996) Utilization of red mud exhausted from Alumina production industry. Shigen-to-Sozai 112(3):131–139. https://doi.org/10.2473/shigentosozai.112.131

15. Liu Y, Naidu R (2014) Hidden values in bauxite residue (red mud): Recovery of metals. Waste Management 34:2662–2673. https://doi.org/10.1016/j.wasman.2014.09.003

16. Miller J, Irgens A (1974) Alumina production by the Pedersen process─history and future. In: Donaldson D, Raahauge B E (ed) Essential Readings in Light Metals pp.977–982. https://doi.org/10.1007/978-3-319-48176-0_135

17. Hignett T P (1947) Production of Alumina from clay by a modified Pedersen process. Industrial & Engineering Chemistry 39(8):1052–1060. https://doi.org/10.1021/ie50452a028

18. ENSUREAL: Ensuring Zero Waste Production of Alumina in Europe, https://ensureal.eu/. Accessed 20 Decenber 2022

19. Sellaeg H, Kolbeinsen L, Safarian J (2017) Iron separation from Bauxite through smelting-reduction process. Light Metals 2017:127–135. https://doi.org/10.1007/978-3-319-51541-0_19

20. Azof F I, Yang Y, Panias D, Kolbeinsen L, Safarian J (2019) Leaching characteristics and mechanism of the synthetic calcium-alminate slags for alumina recovery. Hydrometallurgy 185:273–290. https://doi.org/10.1016/j.hydromet.2019.03.006

21. Ken M (2002) Decomposition Methods of Sparingly soluble Materials. In: Japan Society for Analytical Chemistry (ed), Bunseki 326:60–66

22. Koichi C, Akitoshi O, Hidekazu M, Kazuo O, Tomohiro N, Eiji F, Junji N (2013) ICP Atomic Emission Spectrometry. Kyoritsu, Tokyo

23. Azof F I, Kolbeinsen L, Safarian J (2017) The leachability of Calcium Aluminate phases in slags for the extraction of Alumina. Proceedings of 35th International ICSOBA Conference pp.243–254. https://www.ensureal.com/wp-content/uploads/2017/12/AA13-The-Leachability-of-Calcium-Aluminate-Phases-in-Slags-for-the-Extraction-of-Alumina-ICSOBA-2017.pdf. Accessed on 26 May 2022

24. Chernousov P I, Golubev O V, Petelin A L (2010) Study of Gallium behavior in blast furnace smelting. Metallurgist 54(5–6):285–290. https://doi.org/10.1007/s11015-010-9294-1

25. Garonin S L, Petelin A L, Rykov V V, Chernousov P I, Yusfin Y (2003) Gallium manufacture method. Russian Patent, RU 2247167.

26. Barin I (1995) Thermochemical Data of Pure Substances, Third Edition, Wiley, New York

27. Moore E E, Turchi P E A, Landa A, Söderlind P, Oudot B, Belof J L, Stout S A, Perron A (2019) Development of a CALPHAD thermodynamic database for Pu-U-Fe-Ga Alloys Applied Sciences 9:5040-5064. https://doi.org/10.3390/app9235040

28. Neumann F, Schenck H (1959) Die durch Zusatzelemente bewirkte Aktivitätsänderung von Kohlenstoff in flüssigen Eisenlösungen nahe der Kohlenstoffsättigung. Archiv für das Eisenhüttenwesen 30(8):477–483. https://doi.org/10.1002/srin.195903065

29. Centre for Research in Computational Thermochemistry (CRCT) and GTT-Technologies, FactSage ver. 6.4.

Figure captions

Fig. 1 Flowchart in the Pedersen process for alumina production.

Fig. 2 Photographs of the sample (a) before and (b) after carbothermal reduction in Exp. #1, (c) cross-section of the sample after carbothermal reduction in Exp. #1, and (d) the sample after carbothermal reduction (view from the bottom) in Exp. #2

Fig. 3 XRD patterns of (a) the magnetic powders (#1M) and (b) non-magnetic powders (#1NM) recovered in carbothermal reduction in Exp. #1.

Fig. 4 Transfer ratio and concentration of Ga in the products of the carbothermal reduction (Exp. #1).

Table S-1 Conditions for HCl leaching of the products of carbothermal reduction in Exp. #1

Sample		Magnetic powders (sample #1M)	Non-magnetic powders (sample #1NM)
Mass (g)	Sample	0.501	0.501
	Leachate[a]	10.00	10.03
L/S mass ratio		20.0	20.0

a: Leachate: 2.58 mol L^{-1} HCl

Table S-2 Conditions for HCl leaching of the products of carbothermal reduction in Exp. #2

		Metal			Slag
		#2-1	#2-2	#2-3	
Mass (g)	Sample	0.493	0.498	0.492	0.501
	Leachate[a]	10.01	10.01	10.03	10.03
L/S mass ratio		20.3	20.1	20.4	20.0

a : Leachate: 2.58 mol L^{-1} HCl

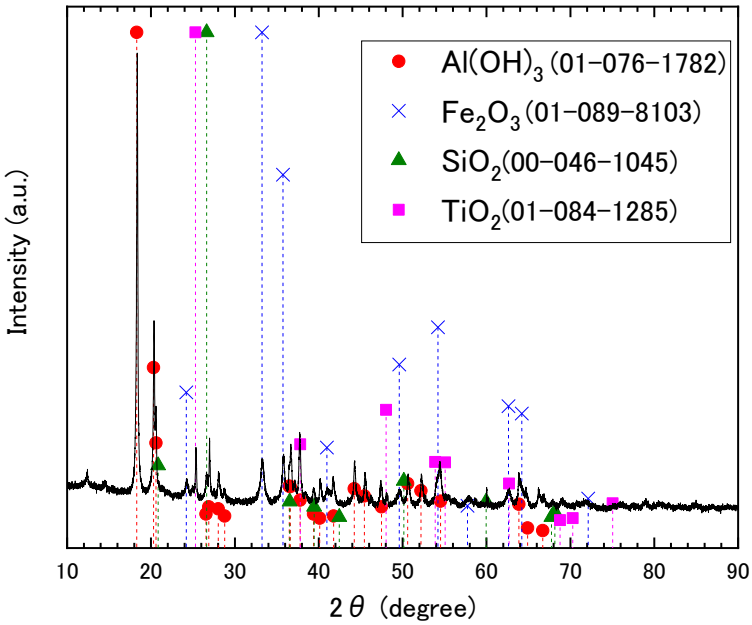

Figure S-1 XRD pattern of the used bauxite.